

# Real-time optoacoustic monitoring of vascular damage during photodynamic therapy treatment of tumor

Liangzhong Xiang

Da Xing

Huaimin Gu

Diwu Yang

Sihua Yang

Lvming Zeng

Wei R. Chen

South China Normal University  
MOE Key Laboratory of Laser Life Science  
and Institute of Laser Life Science  
Guangzhou 510631 China

**Abstract.** The optoacoustic technique is a noninvasive imaging method with high spatial resolution. It potentially can be used to monitor anatomical and physiological changes. Photodynamic therapy (PDT)-induced vascular damage is one of the important mechanisms of tumor destruction, and real-time monitoring of vascular changes can have therapeutic significance. A unique optoacoustic system is developed for neovascular imaging during tumor phototherapy. In this system, a single-pulse laser beam is used as the light source for both PDT and for concurrently generating ultrasound signals for optoacoustic imaging. To demonstrate its feasibility, this system is used to observe vascular changes during PDT treatment of chicken chorioallantoic membrane (CAM) tumors. The photosensitizer used in this study is protoporphyrin IX (PpIX) and the laser wavelength is 532 nm. Neovascularization in tumor angiogenesis is visualized by a series of optoacoustic images at different stages of tumor growth. Damage of the vascular structures by PDT is imaged before, during, and after treatment. Rapid, real-time determination of the size of targeted tumor blood vessels is achieved, using the time difference of positive and negative ultrasound peaks during the PDT treatment. The vascular effects of different PDT doses are also studied. The experimental results show that a pulsed laser can be conveniently used to hybridize PDT treatment and optoacoustic imaging and that this integrated system is capable of quantitatively monitoring the structural change of blood vessels during PDT. This method could be potentially used to guide PDT and other phototherapies using vascular changes during treatment to optimize treatment protocols, by choosing appropriate types and doses of photosensitizers and doses of light. © 2007 Society of Photo-Optical Instrumentation Engineers. [DOI: 10.1117/1.2437752]

**Keywords:** optoacoustic imaging; photodynamic therapy; chicken chorioallantoic membrane tumor; vasculature damage; pulsed laser.

Paper 06201R received Jul. 28, 2006; revised manuscript received Oct. 4, 2006; accepted for publication Oct. 22, 2006; published online Feb. 2, 2007.

## 1 Introduction

Photodynamic therapy (PDT) can be used as a stand-alone modality or in combination with chemotherapy, surgery, radiation therapy, or other new methods, such as antiangiogenic therapy.<sup>1-3</sup> In PDT, a photosensitizing drug is usually administered systemically, and over time it becomes preferentially retained in tumor tissue. When the ratio of photosensitizer accumulation in cancerous tissue versus surrounding normal tissue is optimal, the tumor is exposed to an appropriate light dose, at a selected wavelength coinciding with the absorption peak of the photosensitizer. Photoexcitation of sensitizer molecules, followed by energy transfer to molecular oxygen, leads to the generation of short-lived reactive oxygen species (ROS) that causes oxidative damage to intracellular target molecules.<sup>1-3</sup> Experimental results suggest that PDT can dam-

age blood vessels in the tumor, thereby preventing the cancer from receiving necessary nutrients.<sup>4,5</sup> Thus, in vascular acting PDT, the vascular damage pathway is widely considered to be a prominent mechanism for tumor destruction.<sup>1,4</sup>

Currently there are several *in vivo* techniques for assessing changes in tumor vasculature, but they all have different limitations. Positron emission tomography (PET) scanning often involves contrast agents.<sup>6</sup> Methods based on magnetic resonance imaging (MRI) can provide spatial maps of vessels, but are limited in temporal and spatial resolutions.<sup>7</sup> Optical Doppler tomography (ODT) is able to determine<sup>8</sup> both vessel size and intraluminal blood flow during PDT. However, ODT suffers from strong light scattering in dermal and subdermal tissues, hence resulting in limited tissue penetration depth and low resolution.

Due to technical limitations of available modalities, transient vascular changes are difficult to observe so that the mechanism(s) underlying vascular effects have not been com-

Address all correspondence to: Da Xing, South China Normal University, MOE Key Laboratory for Laser Life Science and Institute of Laser Life Science, Guangzhou 510631 China; Tel: +86-20-8521-0089; Fax: +86-20-8521-6052; E-mail: xingda@scnu.edu.cn

pletely understood. Therefore, a noninvasive, simple method providing both high-resolution and high-contrast images would be beneficial in investigations of vascular effect induced by PDT.

Optoacoustic imaging combines advantages of both ultrasound imaging and optical imaging, to provide high-ultrasonic-resolution and high-optical-contrast tissue images. Recently, optoacoustic imaging has become a popular research subject and has been suggested as a new technique for noninvasive imaging of blood vessels and tumors.<sup>9,10</sup>

The optoacoustic technique is based on the generation of acoustic waves when pulsed light is absorbed by tissue chromophores such as haemoglobin in blood. The induced temperature rise generates a thermoelastic pressure transient.<sup>11–13</sup> The amplitude of the generated ultrasound is dependent on the amount of absorbed light, determined by the local energy fluence and the optical absorption coefficient of the target tissue. Measurement of this pressure transient using piezoelectric sensors is the commonly used method in optoacoustic imaging. The resulting image of the absorber distribution can be used for the quantification of blood vessel size or the vessel density.

The chicken chorioallantoic membrane (CAM) tumor model is an ideal system for *in vivo* studies of PDT-induced vascular damage and for the assessment of angiogenic activity.<sup>14,15</sup> The CAM has a well-vascularized chorioallantoic membrane of fertilized chicken eggs and presents an attractive *in vivo* model. The CAM system has been used to study both the growth and neovascularization of a variety of implanted tumor nodules or tumor cell suspensions.<sup>16,17</sup>

We developed a unique optoacoustic imaging system to monitor the vascular damage during PDT treatment using the CAM tumor model. In this system, a single pulsed laser serves two purposes concurrently: a light source for PDT irradiation and a light source for ultrasound generation. We obtained optoacoustic images of CAM vasculature and quantitatively determined target blood vessel size during PDT treatment. We also investigated the relationship between the vessel damage and PDT dose.

## 2 Materials and Methods

### 2.1 CAM Preparation

In our experiments, fertilized eggs were purchased from Guangdong Academy of Agriculture Science (Guangzhou, China). The eggs were placed in a hatching incubator at 37 °C and 60% humidity. On day 3, while incubation being continued in a static incubator, a 1.5 × 2 cm window was cut into the shell, exposing the CAM.

### 2.2 Implantation of Tumor Cells in CAM

C8161, a highly invasive and spontaneously metastatic human melanoma cell line, was obtained from the Medical School of Jinan University (Guangzhou, China). Cells were maintained in a 1:1 mixture of Dulbecco's modified Eagle's medium supplemented with 10% fetal bovine serum (Invitrogen, New Zealand) and 1- $\mu$ g/ml puromycin (Gibco BRL). The cells were cultured at 37 °C in humidified air with 5% CO<sub>2</sub>. At a density of 70% confluence, cells were removed from the incubator and left at room temperature for approximately 20 min. The resultant cell clusters (consisting of approxi-

mately 10 cells) were transferred to a Petri dish and grown to tumor spheroids of approximately 1.0 mm diameter. Prior to placement on the CAM, each spheroid was embedded in collagen gel (collagen concentration 2 mg/ml). The collagen disk was typically 3 mm in diameter and 2 mm thick. On day 3 of the egg's incubation, the spheroid/collagen gel was placed on the CAM in close proximity ( $\leq 1$  mm) to a capillary bed.

### 2.3 Photosensitizer

The photosensitizer used in this study was protoporphyrin IX (PpIX), purchased from Aldrich Chem. Co. (St. Louis, Missouri). For the photosensitization reaction, photosensitizer protoporphyrin IX disodium salt (PpIX) was prepared according to the manufacturer's directions to a concentration of 200  $\mu$ M. The stock solution was stored in the dark at 4 °C until needed. PpIX solutions were diluted in phosphate-buffered saline (PBS) to concentrations of 20, 30, and 40  $\mu$ mol/L, respectively. Solutions of PpIX were freshly prepared and protected from light before use. A sensitizer of the desired dose was topically applied on the CAM at day 11 of incubation.

The doses for the experiments were selected based on the experimental trials so as to avoid too high a dose for damage of surrounding tissue and to avoid too low a dose for insufficient PDT effect on the blood vessels.

### 2.4 Integrated PDT Treatment and Optoacoustic Imaging System

The experimental system for optoacoustic imaging and photodynamic therapy is shown in Fig. 1. A Q-switched Nd:YAG laser (LOTIS TII Ltd, Minsk, Belarus) was used to provide 532-nm laser pulses with a full width half maximum (FWHM) value of 6.5 ns, with a repetition rate of 10 Hz. The laser beam was expanded and homogenized to provide an incident energy density of  $< 10$  mJ/cm<sup>2</sup> on the surface of the CAM. It was used for therapeutic irradiation of tumor and simultaneously for generating optoacoustic signal during PDT. The hydrophone (Precision Acoustics Ltd., Dorchester, United Kingdom) for recording the optoacoustic signals has a diameter of 1 mm and a sensitivity of 850 nV/Pa. The transducer, driven by a computer-controlled step motor to scan around the chicken embryo, detected the optoacoustic signals in the imaging plane at each scanning position. A pulse amplifier received the signals from the transducer and transmitted the amplified signals to a digital oscilloscope. One set of data at 200 different positions was taken when the receiver moves over 360 deg. After 200 series of data were recorded, the optoacoustic image was reconstructed with the filtered back projection algorithm.<sup>11</sup>

The hydrophone was also placed in one steady position to provide fast measurement (0.625 Hz) of diameters of targeted blood vessels during PDT treatment.

### 2.5 Principle of Optoacoustic Imaging

Optoacoustic imaging is able to accurately localize the microvascular system because of the large optical absorption differences between blood and dermis.<sup>12</sup> The optical absorption  $A(r)$ , within the sample at a given position  $r$  is<sup>9</sup>

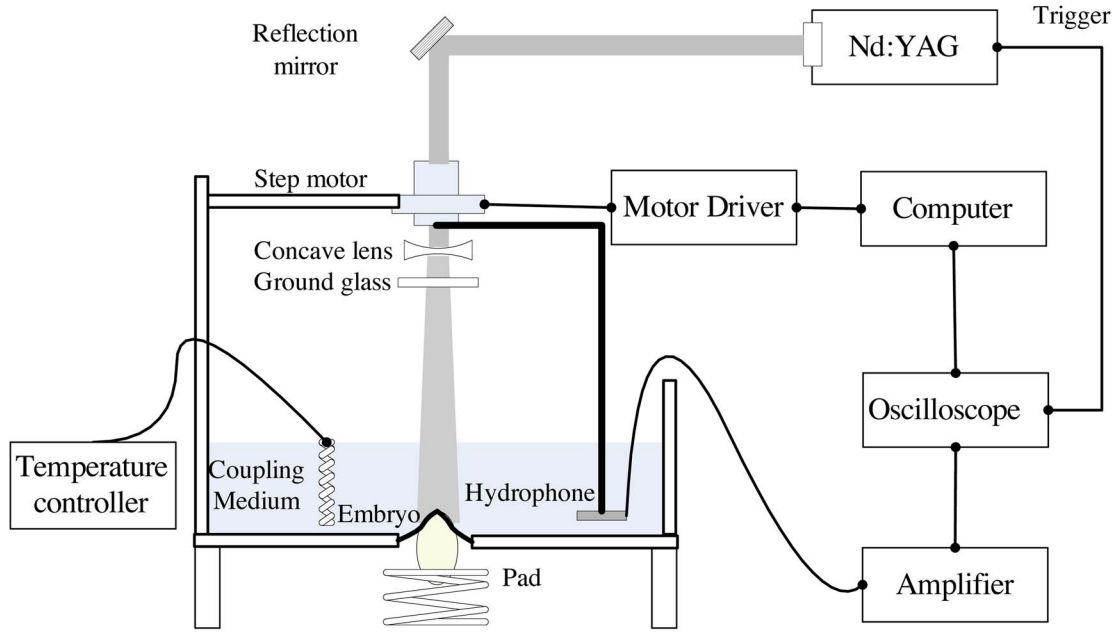


**Fig. 1** Experimental setup of the optoacoustic imaging and PDT system. The 532-nm Nd:YAG pulsed laser is used as the source for treating tumors as well as for generating optoacoustic signals. The laser beam is expanded and homogenized by the concave lens and the ground glass. The hydrophone, driven by a computer-controlled step motor to scan around the chicken embryo, captures the optoacoustic signal during PDT.

$$A(r) = -\frac{r_0^2 C_p}{2\pi v_s^4 \beta} \int_{\theta_0} d\theta_0 \frac{1}{t} \frac{\partial p(r_0, t)}{\partial t} \Bigg|_{t=|r_0-r|/v_s}, \quad (1)$$

where  $C_p$  is the specific heat of the tissue,  $v_s$  is the acoustic speed,  $\beta$  is the thermal coefficient of volume expansion,  $r_0$  is the detector position with respect to the imaging center, and  $p(r_0, t)$  is the optoacoustic signals detected at each scanning angle  $\theta_0$ . According to Eq. (1), the optoacoustic signals can be reconstructed to monitor the neovascularization in tumor angiogenesis and the vascular damage induced by PDT.

The peak-to-peak time ( $\tau_{pp}$ ), the time difference between the occurrences of the positive and negative peaks, of the laser induced pressure transient was used to determine the vessel diameter during PDT. The diameter  $\phi$  of blood vessels can be determined by the relationship<sup>13</sup>

$$\phi = 2c\tau_{pp}, \quad (2)$$

where  $c$  is the speed of sound in blood.

### 2.6 Optoacoustic Tomography of Tumor Neovascularization

During the experiments, the eggs were placed on a vertical adjustable pad. Acoustic coupling between the tissue surface and optoacoustic sensor was obtained by using temperature-controlled water in the tank. Optoacoustic scanning was performed on days 7, 9, and 11 of the incubation. An area of approximately  $1.5 \times 1.5$  cm around the tumor in the CAM was defined by a marker in order to locate the same spot for serial scanning. To prevent hypothermia the embryo was placed on a pad covered by electric heating blanket and water in the tank was maintained at 37 °C, as shown in Fig. 1. The egg was covered by sufficient amounts of ultrasound gel

(Sonogel, Germany) to provide an acoustic coupling medium for the acoustic pressure waves before starting the optoacoustic scanning procedure..

### 2.7 PDT Treatment and CAM Vasculature In Vivo

Eleven days after incubation, the embryos were injected with 100  $\mu$ L of freshly prepared PpIX solution, 30  $\mu$ mol/L. The beam diameter of the pulsed laser radiation at 532 nm was 25 mm to cover the entire tumor area. The CAM was exposed to the laser irradiation with a dose of 4 mJ/cm<sup>2</sup> per pulse and a pulse rate of 10 Hz for 30 min. Light doses were measured with a calibrated photometer (IL1700 Radiometer; International Light, Newburyport, Massachusetts). The interval between the photosensitizer injection and the laser irradiation was 2.5 h. After irradiation, the egg was covered with blackened Parafilm (Aldrich, Buchs, Switzerland) and returned to the incubator. To study the effects of PDT on blood vessels, two types of blood vessels (diameters 70  $\mu$ m  $\pm$  5  $\mu$ m and 140  $\mu$ m  $\pm$  5  $\mu$ m) on the CAMs were monitored. Different PpIX doses, 100  $\mu$ L with concentrations of 20, 30, and 40  $\mu$ mol/L were used. Two different light doses, 2 and 4 mJ/cm<sup>2</sup> per pulse, were also used.

### 2.8 Statistics

A custom software utility was written and incorporated into the computer software package MATLAB (MathWorks, Massachusetts, USA) to analyze and display recorded data. This software enables the reconstruction of the optoacoustic images and the determination of the blood vessel diameter.

At least five CAMs were used for each light and drug dose and the resulting damage was averaged. Data were represented as mean  $\pm$  standard error of measurement (SEM).

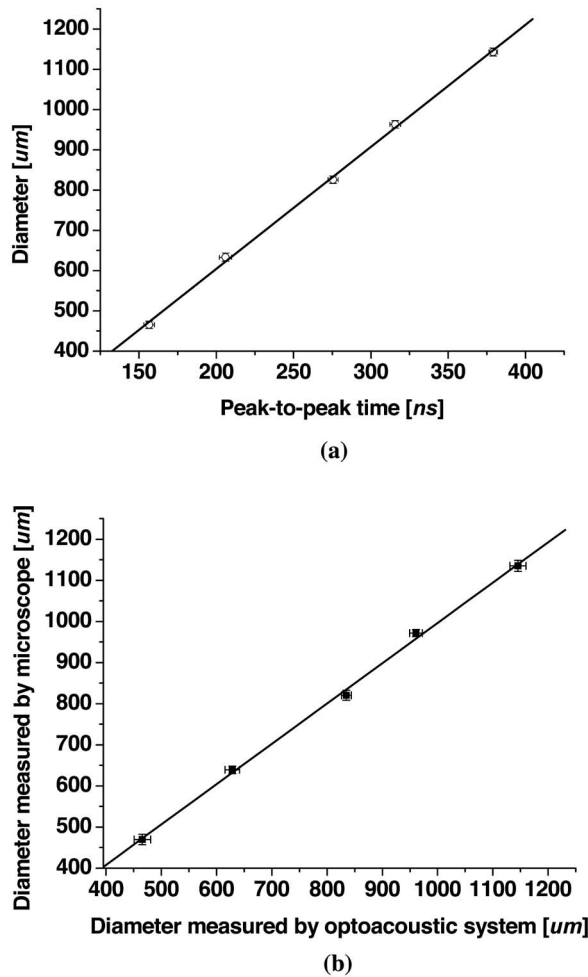


**Fig. 2** Measured artificial blood vessel diameters. (a) A linear relationship between the peak-to-peak times of the pressure transients generated by the laser beam and the sizes of the artificial blood vessels determined by Eq. (2), averaged over five measurements, and (b) linear relationship between microscope-determined vessel size and optoacoustic-system-determined vessel size.

### 3 Results

#### 3.1 Calibration of the Detection System

Artificial blood vessels made of silicon rubber tubes with various diameters, filled with flowing chicken blood (anticoagulated with lithium heparin), were immersed in a 10% Intralipid 10% dilution. The phantom containing the vessel and the Intralipid was immersed in the water. The transducer was also immersed in the water with a perpendicular distance of 55 mm from the vessel. The vessel was illuminated by the laser system as described in the Sec. 2. The resulting peak-to-peak times, plotted as a function of vessel diameters are given in Fig. 2(a). The relation between vessel diameter and peak-to-peak time was determined using Equation (2).

The actual diameters of the artificial vessels, measured with a calibrated microscope, ranged from 0.47 to  $1.14 \pm 0.01$  mm. The vessel sizes were also measured by the optoacoustic system. The results by the two methods agree well, as shown in Figure 2(b).

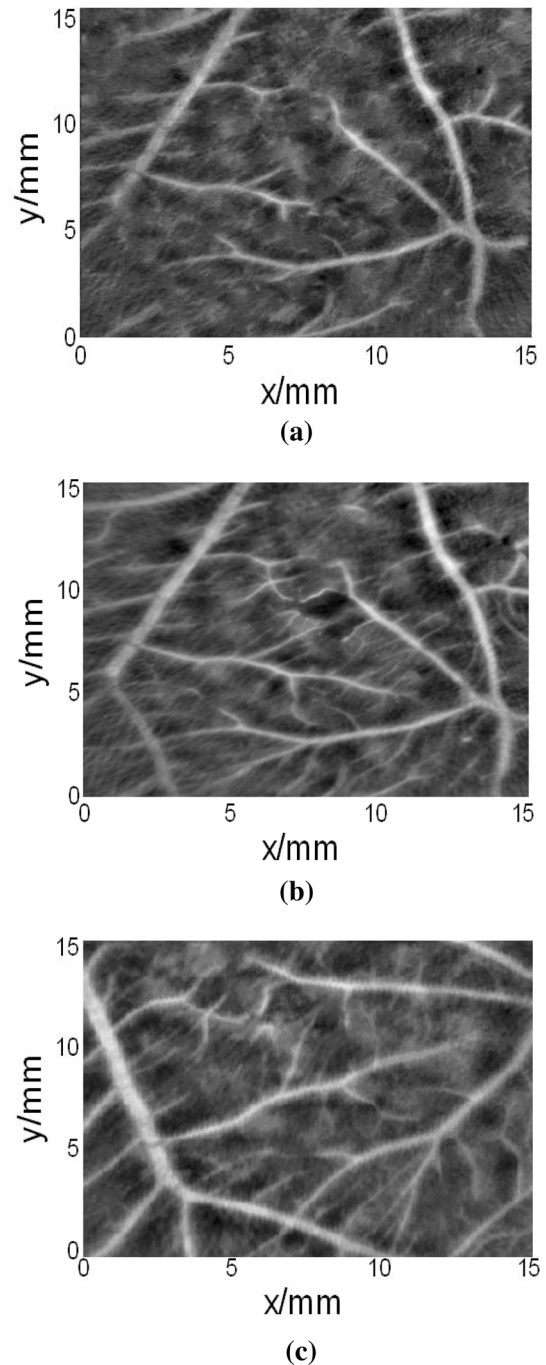


**Fig. 3** Optoacoustic tomography of tumor neovascularization on (a) day 7, (b) day 9, and (c) day 11 of the incubation. The series of images reveal significant size increase of the vessels on the tumor over time.

#### 3.2 Optoacoustic Tomography of Tumor Neovascularization

As shown in Fig. 3, the series of images reveal significant increase of the vessel size on the tumor during the incubation period between day 7 and day 11. On day 7, several blood vessels were seen in the optoacoustic image, suggesting a tumor mass surrounded by developing vessels [Fig. 3(a)]. On day 9, the vessel density has noticeably increased and some

vessels have increased in size [Fig. 3(b)]. The vessel diameters further increased on day 11, as shown in Fig. 3(c).

### 3.3 Observation of Vascular Damage by PDT

On day 11 of the incubation, the sensitizer was topically applied on the chick CAM. The hydrophone was controlled to scan around the CAM to obtain the optoacoustic image. The scanning was performed before, during, and after treatment by light-only irradiation and by PDT with a light dose of  $4 \text{ mJ/cm}^2$  per pulse and a pulse rate of 10 Hz. During the 30-min light irradiation, three complete scans were performed at 10, 20, and 30 min. The CAM vasculature treated by light only is shown in Fig. 4(a); there is no vessel damage during and after the light treatment. Significant vessel damage is observed during and after PDT treatment, as shown in Fig. 4(b). The absence of small vessels in the irradiated field after PDT suggests that they have been completely destroyed.

### 3.4 Measurement of Target Vessel Size During PDT

The transducer was placed in one steady position perpendicular to one of the target vessels on CAM and the optoacoustic signals were measured and recorded in a time interval of 1.6 s (0.625 Hz). Figure 5(a) shows some typical optoacoustic signals from a target vessel at 0, 5, 10, 15, and 20 min during PDT treatment. These signals were used to determine the vessel size. Figure 5(b) shows the size change of the target vessel during the 30-min PDT treatment. The vessel experienced an initial venodilation during the first 2 min of the PDT treatment. Then the vessel diameter decreased monotonically. Results in Fig. 5(b) show a 41.3% decrease in vessel diameter (from 140 to  $57.8 \mu\text{m}$ ) during the 30-min PDT treatment.

### 3.5 Vascular Damage by PDT of Different Doses

Two groups of blood vessels ( $70 \mu\text{m} \pm 5 \mu\text{m}$  and  $140 \mu\text{m} \pm 5 \mu\text{m}$ ) were monitored during PDT treatment with different light doses and PpIX doses as described in Sec. 2. To demonstrate the vessel damage in relation to PDT dose, the optoacoustic signals were recorded in the midpoint of PDT treatment. The results from five CAMs are given in Fig. 6. The results clearly show the dependence of vessel damage on the PDT dose. The PDT apparently had more impact on the smaller vessels [Fig. 6(a)]. At the highest PDT dose ( $40 \mu\text{mol/L}$  and  $4 \text{ mJ/cm}^2$ ) used in our experiments, the  $70\text{-}\mu\text{m}$  vessel was completely destroyed, as shown in Fig. 6(a).

## 4 Discussion

A unique optoacoustic system has been developed for real-time vascular imaging. In this study, this system was used to determine vascular changes during PDT treatment to demonstrate its feasibility. The salient feature of this system is the use of a single pulsed laser as both the therapeutic and the detection light source. This can significantly simplify the imaging-treatment combination system. This unique method utilized the tissue optical absorption differences and the acoustic signal changes to determine the size of the blood vessels during the therapeutic intervention.

The results of the system calibration, as shown in Fig. 2, show the accuracy and the reliability of the system. These

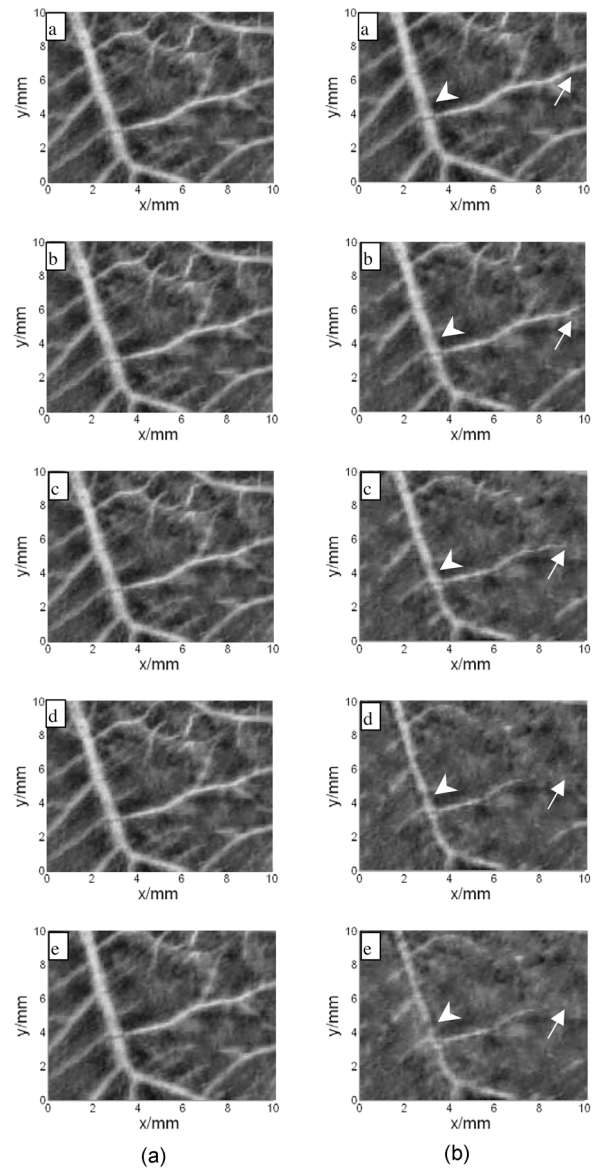


**Fig. 4** Optoacoustic images of vascular structures before, during, and after PDT. (A) Light-only control. The eggs were treated by the light only with a dose of  $4 \text{ mJ/cm}^2$  per pulse and a pulse rate of 10, without application of photosensitizer. The images were taken at (a) 0, (b) 10, (c) 20, and (d) 30 min during light irradiation and (e) after irradiation. (B) PDT treatment [with the application of photosensitizer and the same light dose as in (A)]. The time sequence is the same as in (A). The vessel damage is clearly seen during the PDT treatment in B (b) to (e), while no damage is observed during light-only treatment in A (a) to (e). The arrows point to a small vessel in the irradiated field and the arrowheads point to a large vessel.

results demonstrated that the vessel diameter could be precisely determined by the speed of sound in blood and the peak-to-peak time of pressure transient induced by laser light. The feasibility of the system was further demonstrated by the images of the vascular structures *in vivo*, as shown in Fig. 3. These images of the blood vessel growth in the tumor region show that the imaging system can non-invasively and accurately monitor the tumor neovascularization.

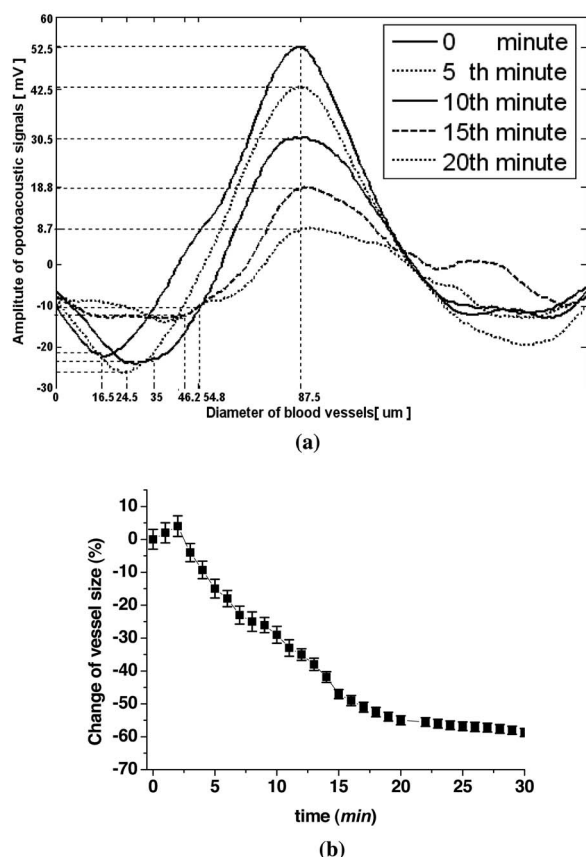


Fig. 5 Real-time determination of the target vessel size of  $140 \mu\text{m}$  diameter using optoacoustic technique during PDT: (a) typical optoacoustic signals from the target vessel at different times and (b) the change of target vessel size during PDT treatment. The concentration of PpIX is  $30 \mu\text{mol/L}$ , and the light dose is  $4 \text{ mJ}/\text{cm}^2$  per pulse.

We obtained high-ultrasonic-resolution and high-optical-contrast tissue images during PDT, to further demonstrate the system's ability in directly observing vascular damages. Figure 4 shows the vascular effects due to the treatment by light only and by PDT before, during, and after the 30-min irradiation. The vascular structure remained intact under the treatment of light [Fig. 4(a)], while the combination of photosensitizer and light irradiation resulted in significant blood vessel damages [Fig. 4(b)]. Our findings indicate that the vessel diameter decrease monotonically in the therapeutic process, in agreement with previous studies.<sup>18,19</sup>

In our experiment, the optoacoustic signals were measured by a transducer. Several positive and negative peaks could be recorded at one time. One of the positive and negative acoustic peaks induced by a vessel was sorted out as a target signals to analyze the change of the vessel diameter. The size of the blood vessel determined using the optoacoustic signals decreased during PDT, as shown in Fig. 5(a). It is apparent that the decrease of the optoacoustic amplitude is related to the decrease of blood perfusion during PDT. This decrease corresponds well with the change of the vessel size [Fig. 5(b)]. Rapid and substantial reductions in tissue oxygenation can also occur during illumination by direct utilization of oxygen during the photochemical generation of reactive oxygen spe-

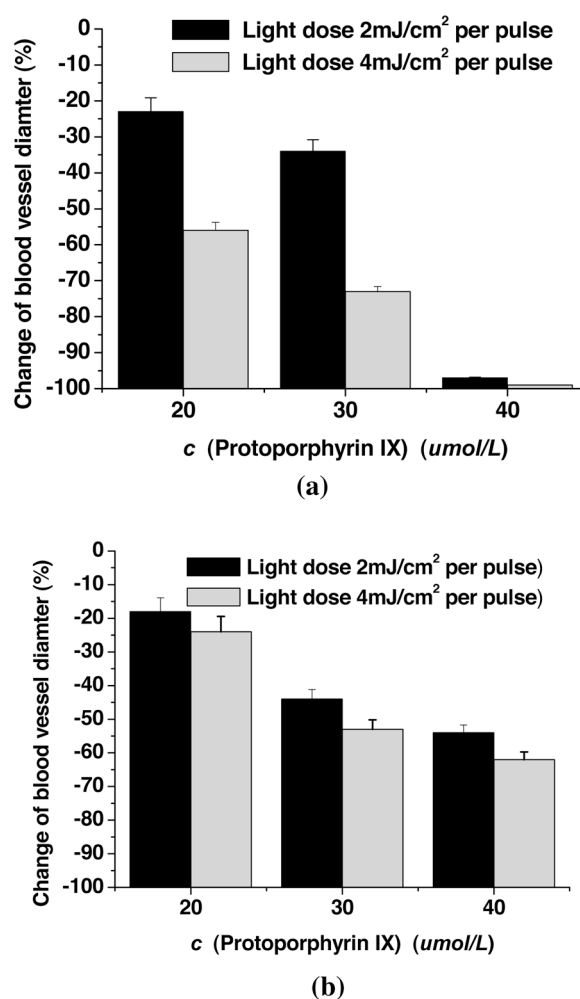


Fig. 6 Vascular damage by PDT of different doses. The concentrations of PpIX are 20, 30, and  $40 \mu\text{mol/L}$ ; the light doses are 2 and  $4 \text{ mJ}/\text{cm}^2$  per pulse. (a) The size change in target vessels of  $70 \mu\text{m} \pm 5 \mu\text{m}$  diameter and (b) the size change in target vessels of  $140 \mu\text{m} \pm 5 \mu\text{m}$  diameter. Bars,  $\pm$  SEM.

cies. Studies have shown that the amplitude of optoacoustic signal may be related to total hemoglobin concentration in blood vessel. Histologic and microscopic observations in various animal models have shown that PDT leads to destructive vascular effects such as thrombosis, thromboxane release by activated platelets, endothelial cell membrane damage, or vascular leakage and constriction. One important aim of PDT is to cause destruction of the microvasculature in and around the tumors.<sup>1,3,20,21</sup>

With the aid of the peak-to-peak time of the laser-induced pressure transient, the axial vessel diameter can be determined without the need of mechanically scanning. This provides a more accurate method to assess the PDT-induced damage to blood vessels than by the damage scales in traditional methods.<sup>22</sup>

We observed the vascular effects of PDT of different doses on blood vessels of different sizes. Figure 6(a) shows the size change of a target vessel of  $75 \mu\text{m}$  diameter under the treatment with three different doses of PpIX. As expected, the damage to the vessels strongly depends on the PDT dose; at

the 40  $\mu\text{mol/L}$  PpIX dose, the vessel was completely destroyed. For a larger vessel (140  $\mu\text{m}$  diameter), the PDT effect is moderate, as shown in Fig. 6(b).

A comparison between irradiation by pulsed wave and by continuous wave with the same average dose showed<sup>23,24</sup> that there was no statistically significant difference in the necrosis of tumor induced by PDT. Studies with high peak pulse powers have demonstrated an increase in the PDT-affected tumor response rate and an increase in the depth of necrosis, compared to the continuous wave irradiation.<sup>23,24</sup> Previous studies also indicated that pulsed laser light at high intensities could cause a transient change in the absorption of the sensitizer by exciting large fractions of the molecules to the excited states within the time of the laser pulse. For sensitizers that have lower extinction coefficients in the upper singlet and triplet states than in the ground state, such population changes are observed as a decrease in the light absorption by the sensitizer. The transient decrease in absorption then allows a higher fraction of the light to be transmitted to the deeper tissue layers; the magnitude of this effect can be estimated from the transmission measurements from thin tissue slices.<sup>23,24</sup> Previous studies showed that a pulsed laser with an incident energy density less than 10  $\text{mJ/cm}^2$  on the skin of a rat head induced an estimated skin temperature increase less than 20 mK. However, that was enough to generate photoacoustic waves for imaging.<sup>9</sup> In our experiments, a pulsed laser with an energy density of 4  $\text{mJ/cm}^2$  was shown to be sufficient to cause PDT effects as well as to produce strong optoacoustic signals for imaging.

PDT sensitizers with fast clearance in the future may provide a highly effective antivasular approach to tumor therapy. Due to the fast clearance, tissue illumination must take place shortly after, or even during, photosensitizer administration. Optoacoustic imaging can be used to guide the tumor positioning before photosensitizer application, providing a significant advantage to enable drug and light administration in a relatively short, single treatment session. Moreover, when the maximum absorption spectrum of new photosensitizers, such as Tookad<sup>®</sup>, is at a longer wavelength (around 760 nm), the light can penetrate deeper into the tissue, enabling the treatment of deep tumors.<sup>25,26</sup> Optoacoustic imaging has a significant advantage over conventional optical methods with far less scattering. It can, consequently, provide deep imaging greater than 5 cm in chicken breast tissue.<sup>27</sup> Therefore, the optoacoustic imaging system can be an effective means for monitoring and evaluating the vascular damage efficacy by using longer excitation wavelength photosensitizers and a longer wavelength laser.

Our new optoacoustic system involves only a single-element ultrasonic transducer. The total acquisition time for one optoacoustic time trace, consisting of 16 averages and including the data transfer from the oscilloscope to the computer, was about 1.6 s at each position. For a  $2\pi$  angular scan with a step size of 1.8 deg, the image acquisition time is about 5 min. In the future, the reduction of the scanning time will be realized by using an array of simultaneously sampled acoustic detectors and a laser with a higher pulse rate.<sup>28,29</sup>

It is known that the biology of cancer varies from tumor to tumor and from patient to patient. Thus, there is a need for an *in vivo* assay enabling rapid assessment of tumor response to

PDT to determine optimal PDT parameters on an individual patient basis. Our *in vitro* and pilot *in vivo* experiments demonstrate that the optoacoustic technique has the potential to provide continuous, accurate, and real-time measurement of the vascular changes during PDT. The ability of the optoacoustic technique to monitor the vascular effect during PDT conveniently and accurately recommends its incorporation into clinical trials of antivasular therapies.

Optoacoustic tomography can provide both high-resolution and high-tissue-contrast images to quantify changes in vessel morphology as well as tumor development in early tumor reproducibility. In particular, this feature makes optoacoustic tomography a promising new tool in tumor angiogenesis research. Furthermore, noninvasive assessment of the extent of tumor vasculature is important in clinical evaluation of the tumor development and treatment.

To the best of our knowledge this is the first time that optoacoustic tomography was used to monitor the photodynamic therapy treatment of tumor *in vivo*. This paper demonstrates that optoacoustic technique is a noninvasive means for monitoring the antiangiogenic or proangiogenic therapies with high optical contrast and high ultrasonic resolution *in vivo*.

#### Acknowledgments

This research is supported by the National Natural Science Foundation of China (60378043; 30470494) and the Natural Science Foundation of Guangdong Province (015012; 04010394; 2004B10401011). We also acknowledge the technical assistance by Dr. Yanchun Wei and helpful conversations with Dr. Lingrui Zhang. We would like to thank Xuanrong Ji, Hui Wang, Yeqi Lao, and Liming Nie for assistance with the tissue phantom experiments.

#### References

1. D. E. J. G. J. Dolmans, D. Fukumura, and R. K. Jain, "Photodynamic therapy for cancer," *Nature (London)* **5**, 380–387 (2003).
2. H. I. Pass, "Photodynamic therapy in oncology: mechanisms and clinical use," *J. Natl. Cancer Inst.* **85**, 443–456 (1993).
3. T. J. Dougherty, C. J. Gomer, B. W. Henderson, G. Jori, D. Kessel, M. Korbelik, J. Moan, and Q. Peng, "Photodynamic therapy," *J. Natl. Cancer Inst.* **90**, 889–905 (1998).
4. W. M. Star, H. P. Marijnissen, A. E. van den Berg-Blok, J. A. Versteeg, K. A. Franken, and H. S. Reinhold, "Destruction of rat mammary tumor and normal tissue microcirculation by hematoporphyrin derivative photoradiation observed *in vivo* in sandwich observation chambers," *Cancer Res.* **46**, 2532–2540 (1986).
5. D. E. J. G. J. Dolmans, A. Kadambi, J. S. Hill, C. A. Waters, B. C. Robinson, J. P. Walker, D. Fukumura, and R. K. Jain, "Vascular accumulation of a novel photosensitizer, MV6401, causes selective thrombosis in tumor vessels after photodynamic therapy," *Cancer Res.* **62**, 2151–2156 (2002).
6. D. R. Collingridge, V. A. Carroll, M. Glaser, E. O. Aboagye, S. Osman, O. C. Hutchinson, H. Barthel, S. K. Luthra, F. Brady, R. Bicknell, P. Price, and A. L. Harris, "A novel tracer for imaging vascular endothelial growth factor *in vivo* using positron emission tomography," *Cancer Res.* **62**, 5912–5919 (2002).
7. D. S. Williams, J. A. Detre, J. S. Leigh, and A. P. Koretsky, "Magnetic resonance imaging of perfusion using spin inversion of arterial water," *Proc. Natl. Acad. Sci. U.S.A.* **89**, 212–216 (1992).
8. A. Major, S. Kimel, S. Mee, T. E. Milner, D. J. Smithies, S. M. Srinivas, Z. Chen, and J. S. Nelson, "Microvascular photodynamic effects determined *in vivo* using optical Doppler tomography," *IEEE J. Sel. Top. Quantum Electron.* **5**(4), 1168–1175 (1999).
9. X. Wang, Y. Pang, G. Ku, X. Xie, G. Stoica, and L. V. Wang, "Non-invasive laser-induced photoacoustic tomography for structural and functional *in vivo* imaging of the brain," *Nat. Biotechnol.* **21**(7), 803–806 (2003).

10. S. L. Jacques, J. A. Viator, and G. Paltauf, "Photoacoustic imaging of tissue blanching during photodynamic therapy of esophageal cancer," *Proc. SPIE* **3916**, 322–330 (2000).
11. D. Yang, D. Xing, H. Gu, Y. Tan, and L. Zeng, "Fast multielement phase-controlled photoacoustic imaging based on limited-field-filtered back-projection algorithm," *Appl. Phys. Lett.* **87**, 194101 (2005).
12. R. I. Siphanto, K. K. Thumma, R. G. M. Kolkman, T. G. van Leeuwen, F. F. M. de Mul, J. W. van Neck, L. N. A. van Adrichem, and W. Steenberg, "Serial noninvasive photoacoustic imaging of neovascularization in tumor angiogenesis," *Opt. Express*, **13**(1), 89–95 (2004).
13. R. G. M. Kolkman, J. H. G. M. Klaessens, E. Hondebrink, J. C. W. Hopman, F. F. M. de Mul, W. Steenberg, J. M. Thijssen, and T. G. van Leeuwen, "Photoacoustic determination of blood vessel diameter," *Phys. Med. Biol.* **49**, 4745–4756 (2004).
14. M. J. Hammer-Wilson, L. Akian, J. Espinoza, S. Kimel, and M. W. Berns, "Photodynamic parameters in the chick chorioallantoic membrane (CAM) bioassay for topically applied photosensitizers," *J. Photochem. Photobiol., B* **53**, 44–52 (1999).
15. V. Gottfried, E. S. Lindenbaum, and S. Kimel, "Vascular damage during PDT as monitored in the chick chorioallantoic membrane," *Int. J. Radiat. Biol.* **60**(1–2), 349–354 (1991).
16. D. Knight, D. Ausprunk, D. Tapper, and J. Folkman, "Avascular and vascular phases of tumor growth in the chick embryo," *Br. J. Cancer* **35**, 347–356 (1977).
17. I. Ishiwata, C. Ishiwata, M. Soma, I. Ono, T. Nakaguchi, and H. Ishikawa, "Tumor angiogenic activity of gynecologic tumor cell lines on the chorioallantoic membrane," *Gynecol. Oncol.* **29**, 87–93 (1988).
18. M. S. Gee, H. M. Saunders, J. C. Lee, J. F. Sanzo, and W. Timothy, "Doppler ultrasound imaging detects changes in tumor perfusion during antivasular therapy associated with vascular anatomic alterations," *Cancer Res.* **61**, 2974–2982 (2001).
19. V. Gottfried, R. Davidi, C. Averbuj, and S. Kimel, "In vivo damage to chorioallantoic membrane blood vessels by porphycene-induced photodynamic therapy," *J. Photochem. Photobiol., B* **30**, 115–121 (1995).
20. I. Y. Petrova, R. O. Esenaliev, Y. Y. Petrov, H.-P. F. Brecht, C. H. Svensen, J. Olsson, D. J. Deyo, and D. S. Prough, "Optoacoustic monitoring of blood hemoglobin concentration: a pilot clinical study," *Opt. Lett.* **30**(13), 1677–1679 (2005).
21. V. H. Fingar, T. J. Wieman, S. A. Wiehle, and P. B. Cerrito, "The role of microvascular damage in photodynamic therapy: the effect of treatment on vessel constriction, permeability, and leukocyte adhesion," *Cancer Res.* **52**(18), 4914–4921 (1992).
22. S. Kimel, L. O. Svaasand, M. Hammer-Wilson, M. J. Schell, T. E. Milner, J. S. Nelson, and M. W. Berns, "Differential vascular response to laser photothermolysis," *J. Invest. Dermatol.* **103**, 693–700 (1994).
23. B. W. Pogue, T. Momma, H. C. Wu, and T. Hasan, "Transient absorption changes in vivo during photodynamic therapy with pulsed-laser light," *Br. J. Cancer* **80**(3–4), 344–351 (1999).
24. C. R. Shea, Y. Hefetz, R. Gilles, J. Wimberly, G. Dalickas, and T. Hasan, "Mechanistic investigation of doxycycline photosensitization by picosecondpulsed and continuous wave laser irradiation of cells in culture," *J. Biol. Chem.* **265**, 5977–5982 (1990).
25. N. V. Koudinova, J. H. Pinthus, A. Brandis, O. Brenner, P. Bendel, J. Ramon, Z. Eshhar, A. Scherz, and Y. Salomon, "Photodynamic therapy with Pd-Bacteriopheophorbide (TOOKAD): successful in vivo treatment of human prostatic small cell carcinoma xenografts," *Int. J. Cancer* **104**(6), 782–789 (2003).
26. Q. Chen, Z. Huang, D. Luck, J. Beckers, P. H. Brun, B. C. Wilson, A. Scherz, Y. Salomon, and F. W. Hetzel, "Preclinical studies in normal canine prostate of a novel palladium-bacteriopheophorbide (WST09) photosensitizer for photodynamic therapy of prostate cancers," *Photochem. Photobiol.* **76**(4), 438–445 (2002).
27. G. Ku and L. V. Wang, "Deep penetrating photoacoustic tomography in biological tissues," *Opt. Lett.* **30**(5), 507–509 (2005).
28. Y. Zeng, D. Xing, Y. Wang, B. Yin, and Q. Chen, "Photoacoustic and ultrasonic co-image with a linear transducer array," *Opt. Lett.* **29**(15), 1760–1762 (2004).
29. D. Yang, D. Xing, Y. Tan, H. Gu, and S. Yang, "Integrative prototype B-scan photoacoustic tomography system based on a novel hybridized scanning head," *Appl. Phys. Lett.* **88**, 174101 (2006).